International Journal of Innovative Research in Advanced Engineering (IJIRAE) ISSN: 2349-2163
Issue 6, Volume 2 (June 2015) www.ijirae.com

Hyperpigmentation Image Segmentation Using Wavelet Networks

Prachi Parakhi
Gogte Institute of Technology, Belgavi

D.A.Kulkarni
Gogte Institute of Technology, Belgavi

Abstract: ***The noninvasive in-vivo skin lesion observation can be achieved by dermoscopy. More often dermoscopy is considered time consuming, subjective and complex due to which, computer-aided diagnosis is gaining the limelight. The most challenging part of analysis is the accurate segmentation of skin lesions. This paper discusses the segmentation of hyperpigmentation images using wavelet networks (WN). Wavelet networks combine the characteristics of both Wavelet Transforms (in denoising, background reduction, and recovery of the characteristic information) and Neural Networks of universal approximation***.

Keywords- wavelet network (WN), dermoscopy, image segmentation, hyperpigmentation, orthogonal least squares

I. INTRODUCTION

A number a diseases affect the human skin, some of which include Eczema, Acne, Lichen planus, Vitiligo. An abnormal appearance of the skin compared to its surrounding skin is known to be the skin lesion. In dermatology hyperpigmentation is the darkening of an area of skin caused by increased melanin. This darkening occurs when an excess of melanin, the brown pigment that produces normal skin color, forms deposits in the skin. Hyperpigmentation can be caused by sun damage, inflammation or other skin injuries. Hyperpigmentation is not only a prevalent condition; it's one that can also be particularly stubborn to treat. In fact, both skin care professionals who face the challenges of treating hyperpigmented skin and the clients who suffer through years of unsuccessful attempts at eliminating it are challenged by this condition. Hyperpigmentation presents no medical threat. However, it can sometimes be a symptom of disease or illness. In computer vision, image segmentation is the process of partitioning a digital image into multiple segments. The goal of segmentation is to simplify and/or change the representation of an image into something that is more meaningful and easier to analyze. Image segmentation is typically used to locate objects and boundaries (lines, curves, etc).

Wavelet Netwoks [1] has been gaining the limelight due to its efficient characteristics. Many of the other artificial intelligence methods like Neural networks flaws have been successfully overcome by Wavelet Networks (WN). Also the classical tool Fourier Transform (FT) limitations can be eliminated by WN. WN structure involves input layer, one or more hidden layers and an output layer. Fig. 1 shows a three layer wavelet network with a hidden layer.

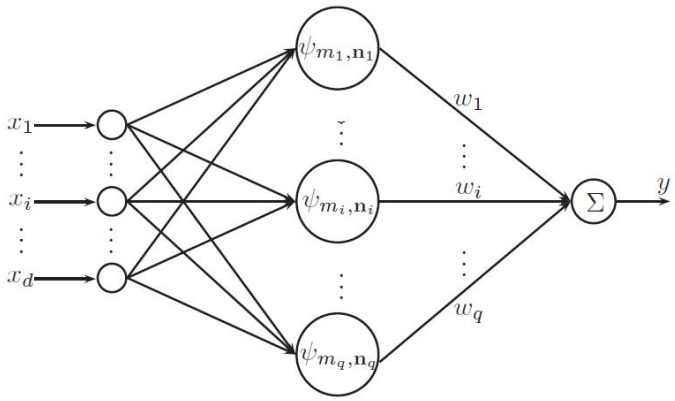

Fig. 1 Wavelet Network structure

Where x=(x^1,….,x^2,…..x^d) T are d inputs, weight coefficients are w_i (i=1,……..,q) , shift and scale parameters are m_i , n_i respectively, dilation and translation versions of mother wavelet ψ are $\psi_{mi,ni}$

$$y = \sum_{i=1}^{q} w_i \psi_{m_i,\mathbf{n}_i}(\mathbf{x}) = \sum_{i=1}^{q} w_i 2^{-m_i d/2} \psi(2^{m_i}\mathbf{x} - \mathbf{n}_i)$$

II. LITERATURE SURVEY

Segmentation of skin images is often considered difficult due to variety of skin types and textures, color, lesion shapes and sizes. Margarida Silveira et al [3] discussed a paper for evaluation of six different segmentation methods of the dermoslesion images, which includes 1) adaptive thresholding 2) gradient vector flow 3) Adaptive snake 4) Level set

method of Chan et al(C-LS) 5) Expectation-Maximization level set method(EM-LS) 6) Fuzzy-Based Split and Merge algorithm (FBSM). Philippe Schmid [4] introduced a paper for dermoscopic image segmentation scheme based on color which employed the Karhunen–Loève transform for the projection of image data onto principal components. The plus point in [4] was non requirement of the prior knowledge regarding the count of objects in the image. Various image processing techniques have been employed for the study and analysis of dermolesions. Prachi Parakhi et al [2] has discussed various methods and its improvements to achieve better accuracy.

M.EminYüksel et al [5] presented segmentation of dermoscopic images with thresholding based on Type-2 Fuzzy Logic whose results were compared with adaptive thresholding and Otsu methods. Jorge S.Marques et al [6] discussed dermoscopic image segmentation based on regions, where the regions in [6] are modelled by probability density functions using the Gaussian mixture followed by Estimation-Maximization (EM) algorithm for the estimation. Howard Zhou et al [7] introduced a paper for the segmentation of dermoscopic images by investigation of spatial constraints using an unsupervised algorithm. This paper [7] considers the growth patterns of the pigmented skin lesions. This paper [7] employs k-means++ algorithm as a variation of the k-means algorithm.

O.Lezoray, M.Revenu et al [8] presented a method for the segmentation of multispectral dermoscopic images by detection of skin lesion borders, resulting Sensitivity=93.62%, Specificity=98.54% and Error Prob=2.79%. David Delgado Gómez et al [9] employs an unsupervised algorithm for the segmentation of dermoscopic images namely Independent Histogram Persuit (IHP). This paper [9] discusses about enhancement of different embedded structures in the images by estimating a set of linear combination of image bands. It resulted in precision close to 97% for the segmentation. Alina Sultana et al [10] introduced a paper that employs preprocessing methods for segmentation of dermolesions for the enhancement of the images in order to obtain better and accurate results. The paper [10] stresses mainly on automated segmentation of the lesion using a mean shift automatic segmentation approach. The steps for preprocessing include contrast enhancement, hair removal, thin blood vessels and skin lines removal.

III. METHODOLOGY

Fixed Grid Wavelet Network (FGWN) in [1] involves weight determination using linear estimation techniques. Its structure can be constructed by employing a ten-stage algorithm. Considering M input-output data as $\{(x^k,y^k)$, k=1, 2,…., M} where d-dimensional input vector is $x^k=[x_1^k,\ldots\ldots\ldots\ldots,x_d^k]$T while X= $[x^1\ldots\ldots x^k\ldots\ldots x^M]$ forms input matrix and Y= $[y^1\ldots\ldots y^k\ldots\ldots y^M]$T forms the output vector.

i. Normalization: Often the WN input data may change within a wide range which leads to lower efficiency of the WN. So as to avoid distributed data, normalization is performed as the first step. In cases of no symbolic data distribution, this step can be omitted.

$$x_{q,\text{new}}^{(k)} = \frac{b-a}{T_k - t_k} x_{q,\text{old}}^{(k)} + \frac{aT_k - bt_k}{T_k - t_k} \qquad 2$$

Where $x_{q,new}^{(k)}$ value is after the normalization process, $x_{q,old}^{(k)}$ value is j^{th} input to the k^{th} sample, [a,b] is the mapping range for the input data.

ii. Selecting the mother wavelet: By using multidimensional single scaling wavelet frame, desirable regularity and easy frame generation can be achieved for which multidimensional Mexican Hat Radial wavelet is employed for WN implementation.

$$\psi(\mathbf{x}) = \eta\|\mathbf{x}\| = (d - \|\mathbf{x}\|^2)\exp(-\|\mathbf{x}\|^2/2). \qquad 3$$

iii. Choose the scale and shift parameters: This step focuses on using minimum and maximum scale levels and shift parameters. Maximum and minimum scale levels as $[m_{min}, m_{max}]$ and shift parameters as $n_j=[n_1,\ldots\ldots n_t,\ldots\ldots n_d]$T , t= 1,……,d and j=1,…..,$\pi_{t=1}^{d}(n_{t,max}- n_{t,min}+1)$ are used.

iv. Formation of wavelet lattice: This step focuses on calculation of wavelet function for all input vectors based on the prior step wavelet parameter space; using a hyper shape as shown in the fig. below

v. Primary Screening: This step involves formation of a set I_k for each scale level from the prior step.

$$I_k = \{(m,\mathbf{n}) : |\psi_{m_i,\mathbf{n}_j}(\mathbf{x})| \geq \epsilon \max_i |\psi_{m_i,\mathbf{n}_j}(\mathbf{x})|\} \qquad 5$$

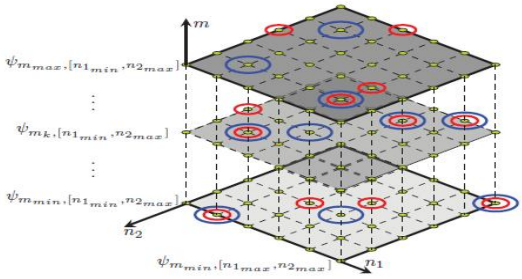

Fig.2 Wavelet Lattice

$$\psi_{m_i,\mathbf{n}_j}(\mathbf{x}) = 2^{-m_i d/2}\psi(2^{m_i}\mathbf{x} - \mathbf{n}_j)$$

Where ε=0.5, typically small positive number. This step helps in selection of the effective wavelets.

v) Secondary screening: In this step a set *I* is constructed based on the wavelets shift and scale parameters from at least two sets from the prior step.

$$I = \{(m,\mathbf{n}) : \text{if}[(m,\mathbf{n}) \in I_{k_r}, (m,\mathbf{n}) \in I_{k_l}] \Rightarrow r \neq l\} \quad 6$$

vi) Formation of wavelet matrix: This step focuses on the matrix calculation for the chosen scale ar t parameters from the prior step and the input vectors.

$$W = \begin{bmatrix} \psi_1(\mathbf{x}^{(1)}) & \dots & \psi_L(\mathbf{x}^{(1)}) \\ \psi_1(\mathbf{x}^{(2)}) & \dots & \psi_L(\mathbf{x}^{(2)}) \\ \vdots & \vdots & \vdots \\ \psi_1(\mathbf{x}^{(M)}) & \dots & \psi_L(\mathbf{x}^{(M)}) \end{bmatrix}.$$

The output vector is then constructed as

$$\mathbf{y} = \sum_{i=1}^{L} w_i \boldsymbol{\psi}_i = W\boldsymbol{\theta}$$

vii) Performing OLS algorithm: The matrix members of prior step can be still redundant as the output information is not considered while the input information is solely considered. The OLS algorithm provides a speedy as well as effective model structure determination approach. The algorithm proceeds in an iterative fashion wherein initially most significant wavelets are selected and the rest non selected wavelets are made orthogonal to the selected once.

viii) Selecting number of wavelons: The nodes that form the hidden layer are wavelons. The system performance index is calculated by selecting an ideal number of wavelons. Until a desired error measure is obtained, the number of wavelons will vary.

$$\text{MSE} = \frac{1}{M}\sum_{k=1}^{M}\left(\hat{y}^{(k)} - y^{(k)}\right)^2.$$

MSE is the index of model performance.

ix) Calculating wavelons weight coefficient: The final step of the algorithm focuses on the weight calculation of wavelons using least-squares method by the equation

QT y = Aθ.

The previous ten steps algorithm is used for the segmentation of dermoscopic images. Firstly the images for building FGWN from the database and normalization process is performed by converting the R, G, & B n the color dermoscopic images into a range [0,1], by which equation (2) becomes:

$$x_{q,\text{new}}^{(k)} = \frac{x_{q,\text{old}}^{(k)} - t_k}{T_k - t_k}$$

where $x_{q,new}^{(k)}$ is the color matrix value after normalization within [0,1] range , t_k is the minimum value and T_k is the maximum value of the matrix. The input, hidden layer and an output are used in FGWN formation and network inputs comprise of three color matrices. The pixel inside and outside the lesion are considered as 0 and 1 respectively as the output. Once the FGWN is formed, the R, G and B values for every pixel are considered as inputs for FGWN and a binary image forms the output of FGWN as shown in fig.2.

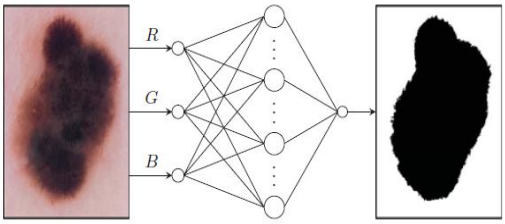

Fig. 3 FGWN for segmentation of dermoscopic image

IV. EXPERIMENTAL RESULTS

This study involves the dataset collected from hospitals and skin diagnosis clinic. The database contains 30 hyperpigmentation images from various parts of the human body. All images are 24-bit RGB color. The ground truth was obtained by manual segmentation performed by skilled dermatologist Dr. Amala Kamat by printing on paper followed by scanning. The proposed algorithm was compared with four other existing algorithms namely Adaptive Thresholding(AT)[11], Gradient Vector Flow(GVF)[12], and Neural Network(NN).

The results for our study are evaluated using PC with Intel i5 and 4GB RAM. The methods are realised using Java with NetBeans IDE. For the purpose of performance evaluation in our experiment, different 11 criteria are considered, which include GA as the ground truth segmentation by the skilled dermatologist, SA as segmentation algorithm result. Both GT and SA are binary images with pixel inside the lesion curve labelled 1 and 0 otherwise. Four parameters define these criteria: True Positive (TP), True Negative (TN), False Positive (FP) and False Negative (FN).

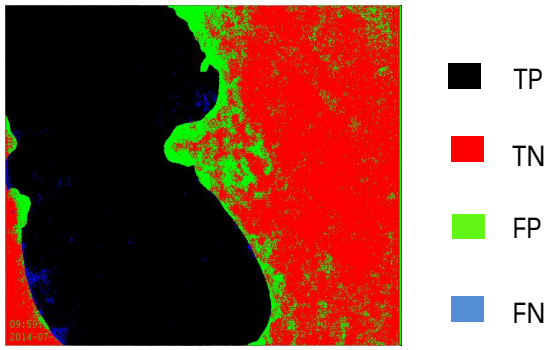

Fig 4 TP depict the number of pixels categorized both by GT and SA as lesion pixels, TN depict the number of pixels categorized both by GT and SA as nonlesion pixels, FP depict the number of pixels where a nonlesion pixel was falsely categorized as part of a lesion by SA, FN is the number of pixels where an lesion pixels was falsely categorized as nonlesion by SA.

	TPR $\frac{TP}{GT}$	TNR $\frac{GT-FP}{GT}$	FPR $\frac{FP}{GT}$	FNR $\frac{FN}{GT}$	Sensitivity $\frac{TP}{TP+FN}$	Specificity $\frac{TN}{TN+FP}$	Accuracy $\frac{TP+TN}{TP+TN+FP+FN}$	Precision $\frac{TP}{TP+FP}$	Similarity $\frac{2TP}{2TP+FN+FP}$	Border Error $\frac{FP+FN}{TP+FN}$	Hamming Distance $\frac{FP+FN}{TN}$
AT	58.65%	100%	0	41.34%	58.65%	100%	79.49%	100%	73.93%	41.34%	40.69%
GVF	12.47%	79.32%	1%	0.2%	98.35%	75.25%	73.75%	84.27%	67.15%	8.32%	2.5%
NN	90.69%	99.55%	0.4%	3.7%	90.69%	99.42%	92.09%	99.53%	92.32%	4.23%	5.50%
FW	98.89%	98.82%	1.17 %	1.10%	98.89%	96.43%	98.28%	98.82%	98.85%	2.28%	7.17%

Table 1 Performance of images from database

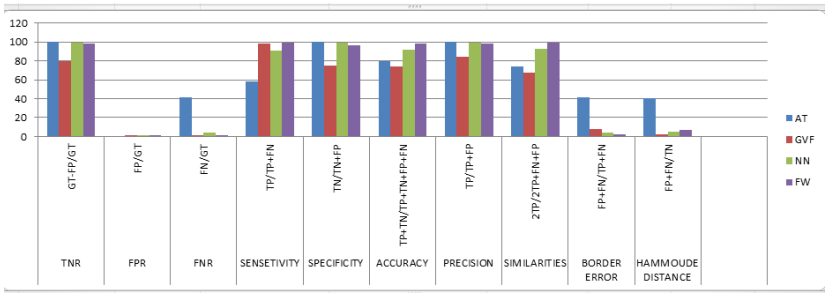

Fig. 5 Graphical representation for Table 1 of all results

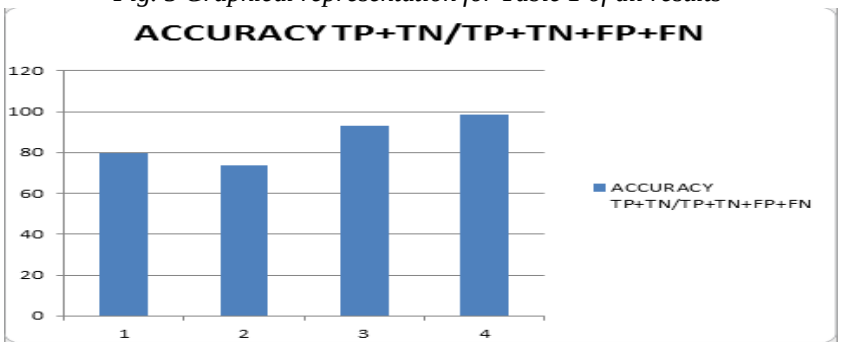

Fig.6 Accuracy results for table 1

CONCLUSION

Our experimental results show better accuracy level for FGWN as compared to other algorithms (AT,GVF,NN). Accuracy= 98.28% has been achieved for the proposed algorithm FGWN. Good contrast images show better results. The proposed segmentation algorithm can be employed in analysis of skin lesion images.

REFERENCES

[1]. Sadri A, Zekri M, Sadri S, Gheissari N, Mokhtari M andKolahdouzan F , APRIL 2013 "*Segmentation of Dermoscopy Images UsingWavelet Networks*", IEEE TRANSACTIONS ON BIOMEDICAL ENGINEERING, VOL. 60, NO. 4, page 1134-1141

[2]. Prachi Parakhi, D.A.Kulkarni "International Journal of Graphics & Image Processing", Vol 5issue 1Feb. 2015 ISSN 2249 – 5452, page 33-38

[3]. Silveira M, Nascimento J. C, S. Marques J, Marçal, A.R.S , Mendonça T, Yamauchi S, Maeda J, and Rozeira J,2009February "*Comparison of Segmentation Methods for Melanoma Diagnosis in Dermoscopy Images*", IEEE JOURNAL OF SELECTED TOPICS IN SIGNAL PROCESSING, VOL. 3, NO. 1, page 35-45

[4]. Schmid P, FEBRUARY 1999 "*Segmentation of Digitized DermatoscopicImagesby Two-Dimensional Color Clustering*" IEEE TRANSACTIONS ON MEDICAL IMAGING, VOL. 18, NO. 2, page 164-171

[5]. EminYuksel M,Borlu M,AUGUST 2009 "*Accurate Segmentation of Dermoscopic Images by ImageThresholding Based on Type-2 FuzzyLogic*" IEEE TRANSACTIONS ON FUZZY SYSTEMS, VOL. 17, NO. 4, page 976-982

[6]. Silveira M, Marques J, 2008, IEEE "Level Set Segmentation of Dermoscopy Images" Instituto Superior T´ecnicoInstituto de Sistemas e Rob´otica, 5th International Symposium on Biomedical imaging from Nano to Macro ISBI, page 173-176

[7]. Zhou H, Chen M, Zouz L, Gass R, Ferris L, Drogowski L, Rehg J, 2008 "Spatially Constrained Segmentation of Dermoscopy Images" *ICBI*, page 1-4.

[8]. Lezoray O, Revenu M, Desvignes M, October2014 ICIP "Graph-based skin lesion segmentation of multispectraldermoscopic images" *IEEE International Conference on Image processing*, page 1-6

[9]. Gómez D, Butakoff C,Ersbøll B, and Stoecker W, JANUARY 2008 "*Independent Histogram Pursuit forSegmentation of Skin Lesions*" IEEE TRANSACTIONS ON BIOMEDICAL ENGINEERING, VOL. 55, NO. 1, page 157-161

[10]. Sultana A, Ciuc M, Radulescu T, Wanyu L, Petrache D, 2012 "Preliminary work on Dermoscopic Lesion Segmentation" *20th European Signal Processing Conference (EUSIPCO 2012) Bucharest, Romania, August 27 – 31, page 2273-2277*

[11]. M. Silveria, J. C. Nascimento, J. S. Marques, A. R. S. Marcal, T. Mendonca, S. Yamauchi, J. Maeda, and J. Rozeira, "Comparison of segmentation methods for melanoma diagnosis in dermoscopy images," IEEE Trans. Signal Process., vol. 3, no. 1, pp. 35–45, Mar. 2009

[12]. B. Erkol, R. H.Moss, R. J. Stanley,W. V. Stoecker, and E. Hva-tum, "Automatic lesion boundary detection in dermoscopy images using gradient vector flow snakes," Skin Res. Technol., vol. 11, no. 1, pp. 17–26, Feb. 2005

